

First measurements of absolute branching fractions of the Ξ_c^+ baryon at Belle

Y. B. Li,⁷¹ C. P. Shen,¹⁰ I. Adachi,^{17,14} J. K. Ahn,³⁸ H. Aihara,⁸⁸ S. Al Said,^{82,35} D. M. Asner,³ H. Atmacan,⁷⁸ T. Aushev,⁵⁶ R. Ayad,⁸² V. Babu,⁸ A. M. Bakich,⁸¹ Y. Ban,⁷¹ V. Bansal,⁶⁹ P. Behera,²⁴ C. Beleño,¹³ M. Berger,⁷⁹ V. Bhardwaj,²¹ B. Bhuyan,²² T. Bilka,⁵ J. Biswal,³² A. Bobrov,^{4,67} A. Bozek,⁶⁴ M. Bračko,^{50,32} T. E. Browder,¹⁶ M. Campajola,^{29,59} L. Cao,³³ D. Červenkov,⁵ V. Chekelian,⁵¹ A. Chen,⁶¹ B. G. Cheon,¹⁵ K. Chilikin,⁴³ H. E. Cho,¹⁵ K. Cho,³⁷ Y. Choi,⁸⁰ S. Choudhury,²³ D. Cinabro,⁹² S. Cunliffe,⁸ S. Di Carlo,⁴¹ Z. Doležal,⁵ D. Dossett,⁵² S. Eidelman,^{4,67,43} D. Epifanov,^{4,67} J. E. Fast,⁶⁹ T. Ferber,⁸ B. G. Fulsom,⁶⁹ R. Garg,⁷⁰ V. Gaur,⁹¹ N. Gabyshev,^{4,67} A. Garmash,^{4,67} A. Giri,²³ P. Goldenzweig,³³ B. Grube,⁸⁴ O. Grzymkowska,⁶⁴ J. Haba,^{17,14} T. Hara,^{17,14} K. Hayasaka,⁶⁶ H. Hayashii,⁶⁰ W.-S. Hou,⁶³ T. Iijima,^{58,57} K. Inami,⁵⁷ G. Inguglia,²⁷ A. Ishikawa,¹⁷ M. Iwasaki,⁶⁸ Y. Iwasaki,¹⁷ W. W. Jacobs,²⁵ S. Jia,² Y. Jin,⁸⁸ D. Joffe,³⁴ K. K. Joo,⁶ A. B. Kaliyar,²⁴ G. Karyan,⁸ Y. Kato,⁵⁷ T. Kawasaki,³⁶ H. Kichimi,¹⁷ C. H. Kim,¹⁵ D. Y. Kim,⁷⁷ H. J. Kim,⁴⁰ K. T. Kim,³⁸ S. H. Kim,¹⁵ K. Kinoshita,⁷ P. Kodyš,⁵ S. Korpar,^{50,32} D. Kotchetkov,¹⁶ P. Križan,^{45,32} R. Kroeger,⁵³ P. Krokovny,^{4,67} T. Kuhr,⁴⁶ R. Kulasiri,³⁴ A. Kuzmin,^{4,67} Y.-J. Kwon,⁹⁴ K. Lalwani,⁴⁸ J. S. Lange,¹¹ I. S. Lee,¹⁵ J. K. Lee,⁷⁵ J. Y. Lee,⁷⁵ S. C. Lee,⁴⁰ C. H. Li,⁴⁴ L. K. Li,²⁶ L. Li Gioi,⁵¹ J. Libby,²⁴ K. Lieret,⁴⁶ D. Liventsev,^{91,17} P.-C. Lu,⁶³ J. MacNaughton,⁵⁴ M. Masuda,⁸⁷ T. Matsuda,⁵⁴ D. Matvienko,^{4,67,43} M. Merola,^{29,59} K. Miyabayashi,⁶⁰ H. Miyata,⁶⁶ R. Mizuk,^{43,55,56} G. B. Mohanty,⁸³ T. J. Moon,⁷⁵ R. Mussa,³⁰ M. Nakao,^{17,14} K. J. Nath,²² M. Nayak,^{92,17} M. Niiyama,³⁹ N. K. Nisar,⁷² S. Nishida,^{17,14} K. Nishimura,¹⁶ S. Ogawa,⁸⁵ H. Ono,^{65,66} Y. Onuki,⁸⁸ P. Pakhlov,^{43,55} G. Pakhlova,^{43,56} B. Pal,³ S. Pardi,²⁹ H. Park,⁴⁰ S.-H. Park,⁹⁴ S. Patra,²¹ S. Paul,⁸⁴ T. K. Pedlar,⁴⁷ R. Pestotnik,³² L. E. Piilonen,⁹¹ V. Popov,^{43,56} E. Prencipe,¹⁹ M. Ritter,⁴⁶ A. Rostomyan,⁸ G. Russo,⁵⁹ D. Sahoo,⁸³ Y. Sakai,^{17,14} M. Salehi,^{49,46} L. Santelj,¹⁷ T. Sanuki,⁸⁶ V. Savinov,⁷² O. Schneider,⁴² G. Schnell,^{1,20} J. Schueler,¹⁶ C. Schwanda,²⁷ A. J. Schwartz,⁷ Y. Seino,⁶⁶ K. Senyo,⁹³ M. E. Sevir,⁵² V. Shebalin,¹⁶ J.-G. Shiu,⁶³ B. Shwartz,^{4,67} F. Simon,⁵¹ A. Sokolov,²⁸ E. Solovieva,⁴³ M. Starič,³² Z. S. Stottler,⁹¹ J. F. Strube,⁶⁹ M. Sumihama,¹² T. Sumiyoshi,⁹⁰ M. Takizawa,^{76,18,73} U. Tamponi,³⁰ K. Tanida,³¹ F. Tenchini,⁸ M. Uchida,⁸⁹ T. Uglov,^{43,56} Y. Unno,¹⁵ S. Uno,^{17,14} Y. Ushiroda,^{17,14} S. E. Vahsen,¹⁶ R. Van Tonder,³³ G. Varner,¹⁶ A. Vinokurova,^{4,67} B. Wang,⁵¹ C. H. Wang,⁶² M.-Z. Wang,⁶³ P. Wang,²⁶ S. Watanuki,⁸⁶ E. Won,³⁸ S. B. Yang,³⁸ H. Ye,⁸ J. Yelton,⁹ J. H. Yin,²⁶ C. Z. Yuan,²⁶ Y. Yusa,⁶⁶ Z. P. Zhang,⁷⁴ V. Zhilich,^{4,67} V. Zhukova,⁴³ and V. Zhulanov,^{4,67}

(Belle Collaboration)

¹University of the Basque Country UPV/EHU, 48080 Bilbao

²Beihang University, Beijing 100191

³Brookhaven National Laboratory, Upton, New York 11973

⁴Budker Institute of Nuclear Physics SB RAS, Novosibirsk 630090

⁵Faculty of Mathematics and Physics, Charles University, 121 16 Prague

⁶Chonnam National University, Kwangju 660-701

⁷University of Cincinnati, Cincinnati, Ohio 45221

⁸Deutsches Elektronen-Synchrotron, 22607 Hamburg

⁹University of Florida, Gainesville, Florida 32611

¹⁰Key Laboratory of Nuclear Physics and Ion-beam Application (MOE) and Institute of Modern Physics, Fudan University, Shanghai 200443

¹¹Justus-Liebig-Universität Gießen, 35392 Gießen

¹²Gifu University, Gifu 501-1193

¹³II. Physikalisches Institut, Georg-August-Universität Göttingen, 37073 Göttingen

¹⁴SOKENDAI (The Graduate University for Advanced Studies), Hayama 240-0193

¹⁵Hanyang University, Seoul 133-791

¹⁶University of Hawaii, Honolulu, Hawaii 96822

¹⁷High Energy Accelerator Research Organization (KEK), Tsukuba 305-0801

¹⁸J-PARC Branch, KEK Theory Center, High Energy Accelerator Research Organization (KEK), Tsukuba 305-0801

¹⁹Forschungszentrum Jülich, 52425 Jülich

²⁰IKERBASQUE, Basque Foundation for Science, 48013 Bilbao

²¹Indian Institute of Science Education and Research Mohali, SAS Nagar, 140306

²²Indian Institute of Technology Guwahati, Assam 781039

²³Indian Institute of Technology Hyderabad, Telangana 502285

²⁴Indian Institute of Technology Madras, Chennai 600036

- ²⁵Indiana University, Bloomington, Indiana 47408
- ²⁶Institute of High Energy Physics, Chinese Academy of Sciences, Beijing 100049
- ²⁷Institute of High Energy Physics, Vienna 1050
- ²⁸Institute for High Energy Physics, Protvino 142281
- ²⁹INFN—Sezione di Napoli, 80126 Napoli
- ³⁰INFN—Sezione di Torino, 10125 Torino
- ³¹Advanced Science Research Center, Japan Atomic Energy Agency, Naka 319-1195
- ³²J. Stefan Institute, 1000 Ljubljana
- ³³Institut für Experimentelle Teilchenphysik, Karlsruher Institut für Technologie, 76131 Karlsruhe
- ³⁴Kennesaw State University, Kennesaw, Georgia 30144
- ³⁵Department of Physics, Faculty of Science, King Abdulaziz University, Jeddah 21589
- ³⁶Kitasato University, Sagami-hara 252-0373
- ³⁷Korea Institute of Science and Technology Information, Daejeon 305-806
- ³⁸Korea University, Seoul 136-713
- ³⁹Kyoto University, Kyoto 606-8502
- ⁴⁰Kyungpook National University, Daegu 702-701
- ⁴¹LAL, Université Paris-Sud, CNRS/IN2P3, Université Paris-Saclay, Orsay
- ⁴²École Polytechnique Fédérale de Lausanne (EPFL), Lausanne 1015
- ⁴³P.N. Lebedev Physical Institute of the Russian Academy of Sciences, Moscow 119991
- ⁴⁴Liaoning Normal University, Dalian 116029
- ⁴⁵Faculty of Mathematics and Physics, University of Ljubljana, 1000 Ljubljana
- ⁴⁶Ludwig Maximilians University, 80539 Munich
- ⁴⁷Luther College, Decorah, Iowa 52101
- ⁴⁸Malaviya National Institute of Technology Jaipur, Jaipur 302017
- ⁴⁹University of Malaya, 50603 Kuala Lumpur
- ⁵⁰University of Maribor, 2000 Maribor
- ⁵¹Max-Planck-Institut für Physik, 80805 München
- ⁵²School of Physics, University of Melbourne, Victoria 3010
- ⁵³University of Mississippi, University, Mississippi 38677
- ⁵⁴University of Miyazaki, Miyazaki 889-2192
- ⁵⁵Moscow Physical Engineering Institute, Moscow 115409
- ⁵⁶Moscow Institute of Physics and Technology, Moscow Region 141700
- ⁵⁷Graduate School of Science, Nagoya University, Nagoya 464-8602
- ⁵⁸Kobayashi-Maskawa Institute, Nagoya University, Nagoya 464-8602
- ⁵⁹Università di Napoli Federico II, 80055 Napoli
- ⁶⁰Nara Women's University, Nara 630-8506
- ⁶¹National Central University, Chung-li 32054
- ⁶²National United University, Miao Li 36003
- ⁶³Department of Physics, National Taiwan University, Taipei 10617
- ⁶⁴H. Niewodniczanski Institute of Nuclear Physics, Krakow 31-342
- ⁶⁵Nippon Dental University, Niigata 951-8580
- ⁶⁶Niigata University, Niigata 950-2181
- ⁶⁷Novosibirsk State University, Novosibirsk 630090
- ⁶⁸Osaka City University, Osaka 558-8585
- ⁶⁹Pacific Northwest National Laboratory, Richland, Washington 99352
- ⁷⁰Panjab University, Chandigarh 160014
- ⁷¹State Key Laboratory of Nuclear Physics and Technology, Peking University, Beijing 100871
- ⁷²University of Pittsburgh, Pittsburgh, Pennsylvania 15260
- ⁷³Theoretical Research Division, Nishina Center, RIKEN, Saitama 351-0198
- ⁷⁴University of Science and Technology of China, Hefei 230026
- ⁷⁵Seoul National University, Seoul 151-742
- ⁷⁶Showa Pharmaceutical University, Tokyo 194-8543
- ⁷⁷Soongsil University, Seoul 156-743
- ⁷⁸University of South Carolina, Columbia, South Carolina 29208
- ⁷⁹Stefan Meyer Institute for Subatomic Physics, Vienna 1090
- ⁸⁰Sungkyunkwan University, Suwon 440-746
- ⁸¹School of Physics, University of Sydney, New South Wales 2006
- ⁸²Department of Physics, Faculty of Science, University of Tabuk, Tabuk 71451
- ⁸³Tata Institute of Fundamental Research, Mumbai 400005
- ⁸⁴Department of Physics, Technische Universität München, 85748 Garching

⁸⁵Toho University, Funabashi 274-8510⁸⁶Department of Physics, Tohoku University, Sendai 980-8578⁸⁷Earthquake Research Institute, University of Tokyo, Tokyo 113-0032⁸⁸Department of Physics, University of Tokyo, Tokyo 113-0033⁸⁹Tokyo Institute of Technology, Tokyo 152-8550⁹⁰Tokyo Metropolitan University, Tokyo 192-0397⁹¹Virginia Polytechnic Institute and State University, Blacksburg, Virginia 24061⁹²Wayne State University, Detroit, Michigan 48202⁹³Yamagata University, Yamagata 990-8560⁹⁴Yonsei University, Seoul 120-749 (Received 26 April 2019; revised manuscript received 1 July 2019; published 12 August 2019)

We present the first measurements of the absolute branching fractions of Ξ_c^+ decays into $\Xi^-\pi^+\pi^+$ and $pK^-\pi^+$ final states. Our analysis is based on a data set of $(772 \pm 11) \times 10^6$ $B\bar{B}$ pairs collected at the $\Upsilon(4S)$ resonance with the Belle detector at the KEKB e^+e^- collider. We measure the absolute branching fraction of $\bar{B}^0 \rightarrow \bar{\Lambda}_c^-\Xi_c^+$ with the Ξ_c^+ recoiling against $\bar{\Lambda}_c^-$ in \bar{B}^0 decays resulting in $\mathcal{B}(\bar{B}^0 \rightarrow \bar{\Lambda}_c^-\Xi_c^+) = [1.16 \pm 0.42(\text{stat.}) \pm 0.15(\text{syst.})] \times 10^{-3}$. We then measure the product branching fractions $\mathcal{B}(\bar{B}^0 \rightarrow \bar{\Lambda}_c^-\Xi_c^+)\mathcal{B}(\Xi_c^+ \rightarrow \Xi^-\pi^+\pi^+)$ and $\mathcal{B}(\bar{B}^0 \rightarrow \bar{\Lambda}_c^-\Xi_c^+)\mathcal{B}(\Xi_c^+ \rightarrow pK^-\pi^+)$. Dividing these product branching fractions by $\bar{B}^0 \rightarrow \bar{\Lambda}_c^-\Xi_c^+$ yields $\mathcal{B}(\Xi_c^+ \rightarrow \Xi^-\pi^+\pi^+) = [2.86 \pm 1.21(\text{stat.}) \pm 0.38(\text{syst.})]\%$ and $\mathcal{B}(\Xi_c^+ \rightarrow pK^-\pi^+) = [0.45 \pm 0.21(\text{stat.}) \pm 0.07(\text{syst.})]\%$. Our result for $\mathcal{B}(\Xi_c^+ \rightarrow \Xi^-\pi^+\pi^+)$ can be combined with Ξ_c^+ branching fractions measured relative to $\Xi_c^+ \rightarrow \Xi^-\pi^+\pi^+$ to set the absolute scale for many Ξ_c^+ branching fractions.

DOI: [10.1103/PhysRevD.100.031101](https://doi.org/10.1103/PhysRevD.100.031101)

In recent decades there has been significant experimental progress on the measurements of the weak decays of charmed baryons [1]. However, given the limited knowledge of the large nonperturbative effects of quantum chromodynamics, it is difficult to reliably calculate the decay amplitudes of charmed baryons from first principles. Furthermore, in exclusive charmed-baryon decays the heavy quark expansion does not work. Hence experimental data are needed to extract the nonperturbative quantities in the decay amplitudes [2–5] and to provide important information to constrain phenomenological models of such decays [6–13].

During the past few years, Belle and BESIII have measured absolute branching fractions of the Λ_c^+ and Ξ_c^0 charmed baryons [14–16]. However, the absolute branching fraction of the remaining member of the charmed-baryon SU(3) flavor antitriplet, the Ξ_c^+ , has not been measured. Branching fractions of Ξ_c^+ decays have been measured relative to the $\Xi^-\pi^+\pi^+$ mode. A measurement of the absolute branching fraction $\mathcal{B}(\Xi_c^+ \rightarrow \Xi^-\pi^+\pi^+)$ is needed to infer the absolute branching fractions of other Ξ_c^+ decays. The comparison of Ξ_c^+ decays with those of Λ_c^+ and Ξ_c^0 can also provide an important test of SU(3) flavor symmetry [17].

Along with the reference mode $\Xi_c^+ \rightarrow \Xi^-\pi^+\pi^+$, $\Xi_c^+ \rightarrow pK^-\pi^+$ is a particularly important decay mode as it is the one most often used to reconstruct Ξ_c^+ candidates at hadron collider experiments, such as LHCb. For example, the decay has been used to study the properties of Ξ_b and to search for higher excited Ξ_b states via $\Xi_b^0 \rightarrow \Xi_c^+\pi^-$ [18,19], to search for new Ω_c^* states in the $\Xi_c^+K^-$ mode [20], to measure the doubly charmed baryon via $\Xi_{cc}^{++} \rightarrow \Xi_c^+\pi^+$ [21], as well as to measure the ratio of fragmentation fractions of $b \rightarrow \Xi_b^0$ relative to $b \rightarrow \Lambda_b^0$ [22,23].

In experiments, the decay $\Xi_c^+ \rightarrow pK^-\pi^+$ has been observed by the FOCUS and SELEX collaborations and the branching fraction ratio is measured to be $\mathcal{B}(\Xi_c^+ \rightarrow pK^-\pi^+)/\mathcal{B}(\Xi_c^+ \rightarrow \Xi^-\pi^+\pi^+) = 0.21 \pm 0.04$ [1,24–26]. A few models have been developed to predict the decay rates of Ξ_c^+ . For example, the $\mathcal{B}(\Xi_c^+ \rightarrow \Xi^-\pi^+\pi^+)$ has been predicted to be $(1.47 \pm 0.84)\%$ based on the SU(3) flavor symmetry [27]. Theory predicts $\mathcal{B}(\Xi_c^+ \rightarrow pK^-\pi^+)$ to be $(2.2 \pm 0.8)\%$ based on the measured ratio $\mathcal{B}(\Xi_c^+ \rightarrow p\bar{K}^{*0})/\mathcal{B}(\Xi_c^+ \rightarrow pK^-\pi^+)$ and the U -spin symmetry that relates $\Xi_c^+ \rightarrow p\bar{K}^{*0}$ and $\Lambda_c^+ \rightarrow \Sigma^+K^{*0}$ [23,28]. The decay $\bar{B}^0 \rightarrow \bar{\Lambda}_c^-\Xi_c^+$, which proceeds via a $b \rightarrow c\bar{c}s$ transition, has been predicted to have a branching fraction of the order of 10^{-3} [29], but there has been no experimental measurement. The world average of the product branching fraction $\mathcal{B}(\bar{B}^0 \rightarrow \bar{\Lambda}_c^-\Xi_c^+)\mathcal{B}(\Xi_c^+ \rightarrow \Xi^-\pi^+\pi^+)$ is $(1.8 \pm 1.8) \times 10^{-5}$ with large uncertainty [1,30,31].

In this paper, we perform an analysis of $\bar{B}^0 \rightarrow \bar{\Lambda}_c^-\Xi_c^+$ with $\bar{\Lambda}_c^-$ reconstructed via its $\bar{p}K^+\pi^-$ decay, and Ξ_c^+ reconstructed both inclusively and exclusively via the

Published by the American Physical Society under the terms of the [Creative Commons Attribution 4.0 International license](https://creativecommons.org/licenses/by/4.0/). Further distribution of this work must maintain attribution to the author(s) and the published article's title, journal citation, and DOI. Funded by SCOAP³.

decay modes $\Xi^- \pi^+ \pi^+$ and $pK^- \pi^+$ [32]. We present first a measurement of the absolute branching fraction for $\bar{B}^0 \rightarrow \bar{\Lambda}_c^- \Xi_c^+$ using a missing-mass technique, which is explained below. For this analysis we fully reconstruct the tag-side B^0 decay. We subsequently measure the product branching fractions $\mathcal{B}(\bar{B}^0 \rightarrow \bar{\Lambda}_c^- \Xi_c^+) \mathcal{B}(\Xi_c^+ \rightarrow \Xi^- \pi^+ \pi^+)$ and $\mathcal{B}(\bar{B}^0 \rightarrow \bar{\Lambda}_c^- \Xi_c^+) \mathcal{B}(\Xi_c^+ \rightarrow pK^- \pi^+)$ without reconstructing the recoiling B^0 decay in the event as the signal decays are fully reconstructed. Dividing these product branching fractions by the result for $\mathcal{B}(\bar{B}^0 \rightarrow \bar{\Lambda}_c^- \Xi_c^+)$ yields the $\mathcal{B}(\Xi_c^+ \rightarrow \Xi^- \pi^+ \pi^+)$ and $\mathcal{B}(\Xi_c^+ \rightarrow pK^- \pi^+)$.

This analysis is based on the full data sample of 711 fb⁻¹ collected at the $\Upsilon(4S)$ resonance by the Belle detector [33] at the KEKB asymmetric-energy e^+e^- collider [34]. To determine detection efficiency and optimize signal event selections, B meson decay events are generated using EVTGEN [35] and Ξ_c^+ inclusive decays are generated using PYTHIA [36]. The events are then processed by a detector simulation based on GEANT3 [37]. Monte Carlo (MC) simulated samples of $\Upsilon(4S) \rightarrow B\bar{B}$ events with $B = B^+$ or B^0 , and $e^+e^- \rightarrow q\bar{q}$ events with $q = u, d, s, c$ at a center-of-mass energy of $\sqrt{s} = 10.58$ GeV are used to examine possible peaking backgrounds.

Selection of signal and $\Lambda \rightarrow p\pi^-$ candidates uses well reconstructed tracks and particle identification as described in Ref. [38]. For the inclusive analysis of the Ξ_c^+ decay, the tag-side B^0 meson candidate, B_{tag}^0 , is reconstructed using a neural network based on a full hadron-reconstruction algorithm [39]. Each B_{tag}^0 candidate has an associated output value O_{NN} from the multivariate analysis, which ranges from 0 to 1. A candidate with larger O_{NN} is more likely to be a true B^0 meson. If multiple B_{tag}^0 candidates are found in an event, the candidate with the largest O_{NN} value is selected. To improve the purity of the B_{tag}^0 sample, we require $O_{\text{NN}} > 0.005$, $M_{\text{bc}}^{\text{tag}} > 5.27$ GeV/ c^2 , and $|\Delta E^{\text{tag}}| < 0.04$ GeV, where the latter two intervals correspond to approximately 3 standard deviations, 3σ . $M_{\text{bc}}^{\text{tag}}$ and ΔE^{tag} are defined as $M_{\text{bc}}^{\text{tag}} \equiv \sqrt{E_{\text{beam}}^2 - (\sum_i \vec{p}_i^{\text{tag}})^2}$ and $\Delta E^{\text{tag}} \equiv \sum_i E_i^{\text{tag}} - E_{\text{beam}}$, where $E_{\text{beam}} \equiv \sqrt{s}/2$ is the beam energy, $(E_i^{\text{tag}}, \vec{p}_i^{\text{tag}})$ is the four-momentum of the B_{tag}^0 daughter i in the e^+e^- center-of-mass system (c.m.s.). $\bar{\Lambda}_c^- \rightarrow \bar{p}K^+\pi^-$ candidates are selected using the same method as in Ref. [16]. A 3σ $\bar{\Lambda}_c^-$ signal region is defined by $|M_{\bar{\Lambda}_c^-} - m_{\bar{\Lambda}_c^-}| < 10$ MeV/ c^2 . Here and throughout the text, M_i represents a measured invariant mass and m_i denotes the nominal mass of the particle i [1].

The mass recoiling against the $\bar{\Lambda}_c^-$ in $\bar{B}^0 \rightarrow \bar{\Lambda}_c^- + X$ is calculated using $M_{\text{tag}}^{\text{recoil}} = \sqrt{(P_{\text{c.m.s.}} - P_{B_{\text{tag}}^0} - P_{\bar{\Lambda}_c^-})^2}$. To improve the recoil-mass resolution we use $M_{\text{tag}}^{\text{recoil}} \equiv M_{B_{\text{tag}}^0}^{\text{recoil}} + M_{B_{\text{tag}}^0} - m_{B^0} + M_{\bar{\Lambda}_c^-} - m_{\bar{\Lambda}_c^-}$. Here, $P_{\text{c.m.s.}}$, $P_{B_{\text{tag}}^0}$, and $P_{\bar{\Lambda}_c^-}$ are four-momenta of the initial e^+e^- system, the

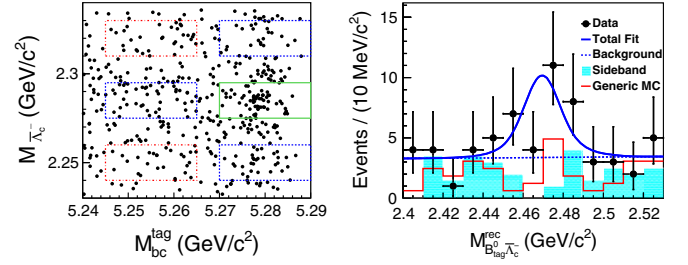


FIG. 1. The distribution of $M_{\text{bc}}^{\text{tag}}$ of the B_{tag}^0 versus $M_{\bar{\Lambda}_c^-}$ for selected $\bar{B}^0 \rightarrow \bar{\Lambda}_c^- \Xi_c^+$ candidates with $\Xi_c^+ \rightarrow$ anything and $\bar{\Lambda}_c^- \rightarrow \bar{p}K^+\pi^-$ (left) and the fit to the $M_{B_{\text{tag}}^0 \bar{\Lambda}_c^-}^{\text{rec}}$ distribution (right).

The solid box shows the selected signal region. The blue dashed and red dash-dotted boxes define the $M_{\text{bc}}^{\text{tag}}$ and $M_{\bar{\Lambda}_c^-}$ sidebands described in the text. The points with error bars are the data in the signal box, the solid blue curve is the best fit, the dashed curve is the fitted background, the cyan shaded histogram is the normalized $M_{\text{bc}}^{\text{tag}}$ and $M_{\bar{\Lambda}_c^-}$ sidebands, the red open histogram is the sum of the MC-simulated contributions for $e^+e^- \rightarrow q\bar{q}$, and $\Upsilon(4S) \rightarrow B\bar{B}$ generic-decay backgrounds with the number of events normalized to the number of events from the normalized $M_{\text{bc}}^{\text{tag}}$ and $M_{\bar{\Lambda}_c^-}$ sidebands.

tagged B^0 meson, and the reconstructed $\bar{\Lambda}_c^-$ baryon, respectively.

Figure 1 (left) shows the distribution of $M_{\text{bc}}^{\text{tag}}$ of the B_{tag}^0 candidates versus $M_{\bar{\Lambda}_c^-}$ of the selected $\bar{B}^0 \rightarrow \bar{\Lambda}_c^- \Xi_c^+$ signal candidates after all selection requirements in the studied Ξ_c^+ mass region of $2.4 < M_{B_{\text{tag}}^0 \bar{\Lambda}_c^-}^{\text{rec}} < 2.53$ GeV/ c^2 . Candidates $\bar{B}^0 \rightarrow \bar{\Lambda}_c^- \Xi_c^+$ are observed in the signal region defined by the solid box. To check possible peaking backgrounds, we define $M_{\text{bc}}^{\text{tag}}$ and $M_{\bar{\Lambda}_c^-}$ sidebands, which are represented by the dashed and dash-dotted boxes. The normalized contribution of the $M_{\text{bc}}^{\text{tag}}$ and $M_{\bar{\Lambda}_c^-}$ sidebands is estimated as being half the number of events in the blue dashed boxes minus one fourth the number of events in the red dash-dotted boxes. The $M_{B_{\text{tag}}^0 \bar{\Lambda}_c^-}^{\text{rec}}$ distribution in the signal and the sideband boxes is shown in Fig. 1 (right).

To extract the Ξ_c^+ signal yields we perform an unbinned maximum likelihood fit to the $M_{B_{\text{tag}}^0 \bar{\Lambda}_c^-}^{\text{rec}}$ distribution. A double-Gaussian function with its parameters fixed to those from a fit to the MC-simulated signal distribution is used to model the Ξ_c^+ signal shape and a first-order polynomial is used for the background shape since we find no peaking background in the $M_{\text{bc}}^{\text{tag}}$ and $M_{\bar{\Lambda}_c^-}$ sideband events. For all the fits described in this paper, the signal and background yields, and the parameters of the background shape are left free. The fit results are shown in Fig. 1 (right).

The fitted number of Ξ_c^+ signal events is $N_{\Xi_c^+} = 18.8 \pm 6.8$. This corresponds to a statistical significance of 3.2σ estimated using $\sqrt{-2 \ln(\mathcal{L}_0/\mathcal{L}_{\text{max}})}$, where \mathcal{L}_0 and \mathcal{L}_{max} are the maximum likelihood values of the fits

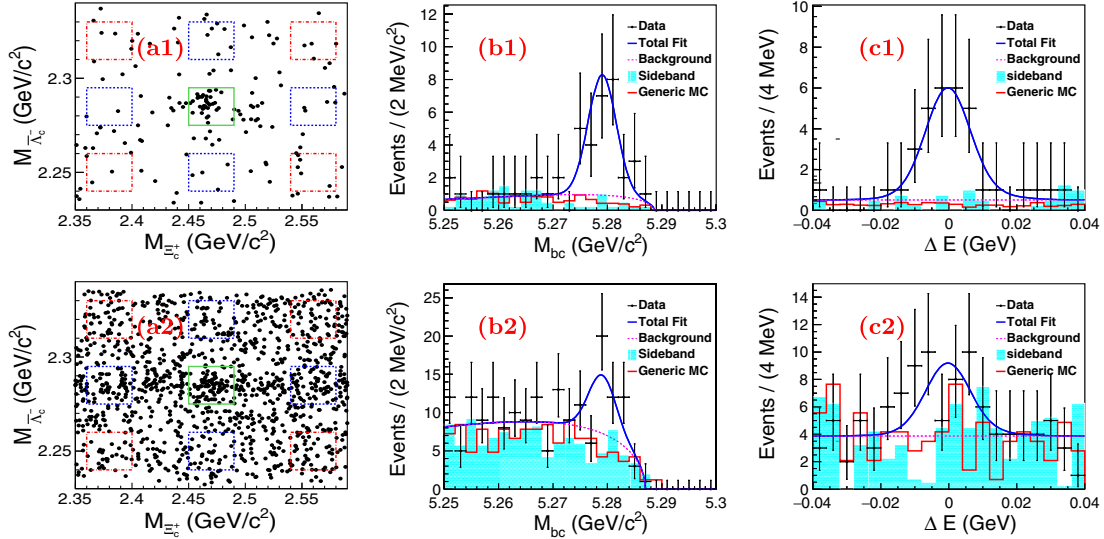


FIG. 2. The distributions of (a) $M_{\Xi_c^+}$ versus $M_{\bar{\Lambda}_c^-}$, and the fits to the (b) M_{bc} and (c) ΔE distributions of the selected $\bar{B}^0 \rightarrow \bar{\Lambda}_c^- \Xi_c^+$ candidates for (b1-c1) the $\Xi_c^+ \rightarrow \Xi^- \pi^+ \pi^+$ and (b2-c2) the $\Xi_c^+ \rightarrow p K^- \pi^+$ decay modes. In plots (a1-a2), the central solid boxes are the signal regions, and the red dash-dotted and blue dashed boxes show the $M_{\Xi_c^+}$ and $M_{\bar{\Lambda}_c^-}$ sidebands used to estimate of the backgrounds (see text). The dots with error bars are the data, the blue solid curves represent the best fits, and the dashed curves represent the fit background contributions. The shaded histograms are the normalized as in the text $M_{\Xi_c^+}$ and $M_{\bar{\Lambda}_c^-}$ sidebands, the red open histograms represent the generic background described in the caption of Fig. 1.

without and with a signal component, respectively. The signal significance becomes 3.1σ once we convolve the likelihood with a Gaussian function whose width equals the total systematic uncertainty. The signal significance found using alternative fits to the $M_{B_{\text{tag}}^{\text{rec}} \bar{\Lambda}_c^-}$ distribution as described in the section on systematic uncertainties, is greater than 3.0σ in all cases. The branching fraction is

$$\begin{aligned} \mathcal{B}(\bar{B}^0 \rightarrow \bar{\Lambda}_c^- \Xi_c^+) &= N_{\Xi_c^+} / [2N_{\bar{B}^0} \epsilon_{\text{inc}} \mathcal{B}(\bar{\Lambda}_c^- \rightarrow \bar{p} K^+ \pi^-)] \\ &= [1.16 \pm 0.42(\text{stat.})] \times 10^{-3}, \end{aligned}$$

where $N_{\bar{B}^0} = N_{\Upsilon(4S)} \mathcal{B}(\Upsilon(4S) \rightarrow B^0 \bar{B}^0)$, $N_{\Upsilon(4S)}$ is the number of $\Upsilon(4S)$ events, and $\mathcal{B}(\Upsilon(4S) \rightarrow B^0 \bar{B}^0) = 0.486$ [1]. The reconstruction efficiency, ϵ_{inc} , is obtained from the MC simulation. The $\mathcal{B}(\bar{\Lambda}_c^- \rightarrow \bar{p} K^+ \pi^-)$ is taken from Ref. [1].

For the analysis of the exclusive Ξ_c^+ decays, we reconstruct Ξ_c^+ from $\Xi^- \pi^+ \pi^+$ with $\Xi^- \rightarrow \Lambda \pi^- (\Lambda \rightarrow p \pi^-)$ and $\Xi^- \rightarrow p K^- \pi^+$ modes, with no B_{tag}^0 . The daughters of the \bar{B}^0 , Ξ_c^+ , and Ξ^- candidates are fit to common vertices. If there is more than one \bar{B}^0 candidate in an event, the one with the smallest $\chi^2_{\text{vertex}}/\text{n.d.f.}$ from the \bar{B}^0 vertex fit is selected. The requirements of $\chi^2_{\text{vertex}}/\text{n.d.f.} < 50, 15,$ and 15 are applied to reconstructed $\bar{B}^0, \Xi_c^+,$ and Ξ^- candidates, respectively, with selection efficiencies above 96%, 95%, and 95%. Ξ^- and Ξ_c^+ signals are defined as $|M_{\Xi^-} - m_{\Xi^-}| < 10 \text{ MeV}/c^2$ and $|M_{\Xi_c^+} - m_{\Xi_c^+}| < 20 \text{ MeV}/c^2$ corresponding to about 3σ . The $\bar{\Lambda}_c^-$ signal interval is the same as in the

inclusive analysis of Ξ_c^+ decays. \bar{B}^0 signal candidates are identified using the beam-constrained mass M_{bc} and the energy difference ΔE . Here, M_{bc} and ΔE are defined as M_{bc}^{tag} and ΔE^{tag} above, but calculated using the momenta of the signal candidate tracks directly.

After the event selections, the distributions of $M_{\Xi_c^+}$ versus $M_{\bar{\Lambda}_c^-}$ in the \bar{B}^0 signal region defined by $|\Delta E| < 0.03 \text{ GeV}$ and $M_{bc} > 5.27 \text{ GeV}/c^2$ corresponding to about 3σ are shown in Figs. 2(a1) and 2(a2). The central solid boxes are the Ξ_c^+ and $\bar{\Lambda}_c^-$ signal regions. The backgrounds from non- Ξ_c^+ and non- $\bar{\Lambda}_c^-$ events are estimated with the $M_{\Xi_c^+}$ and $M_{\bar{\Lambda}_c^-}$ sidebands, represented by the dashed and dash-dotted boxes in Figs. 2(a1) and 2(a2). The normalized contributions from the $M_{\Xi_c^+}$ and $M_{\bar{\Lambda}_c^-}$ sidebands are estimated using half the number of events in the blue dashed boxes minus one fourth the number of events in the red dash-dotted boxes. Figure 2 shows the M_{bc} and ΔE distributions in the Ξ_c^+ and $\bar{\Lambda}_c^-$ signal regions from the selected $\bar{B}^0 \rightarrow \bar{\Lambda}_c^- \Xi_c^+$ candidates with $\Xi_c^+ \rightarrow \Xi^- \pi^+ \pi^+$ (b1-c1) and $\Xi_c^+ \rightarrow p K^- \pi^+$ (b2-c2) decay modes.

We perform a two-dimensional (2D) maximum likelihood fit to the M_{bc} and ΔE distributions to extract the number of $\bar{B}^0 \rightarrow \bar{\Lambda}_c^- \Xi_c^+$ signal events with $\Xi_c^+ \rightarrow \Xi^- \pi^+ \pi^+ / p K^- \pi^+$. For the M_{bc} distribution, the signal shape is modeled using a Gaussian function and the background is described using an ARGUS function [40]. For the ΔE distribution, the signal shape is a double Gaussian and the background is a first-order polynomial. All shape parameters of the signal functions are fixed to the

TABLE I. Summary of the measured Ξ_c^+ branching fractions and ratio (last column), and the corresponding systematic uncertainties in %. For the branching fractions and ratio, the first uncertainties are statistical and the second are systematic.

Observable	Efficiency	Fit	Λ_c decays	B_{tag}	N_{B^0}	Sum	Measured value
$\mathcal{B}(\bar{B}^0 \rightarrow \bar{\Lambda}_c^- \Xi_c^+)$	3.66	10.3	5.3	4.5	1.82	13.1	$(1.16 \pm 0.42 \pm 0.15) \times 10^{-3}$
$\mathcal{B}(\bar{B}^0 \rightarrow \bar{\Lambda}_c^- \Xi_c^+) \mathcal{B}(\Xi_c^+ \rightarrow \Xi^- \pi^+ \pi^+)$	6.24	5.61	5.3	...	1.82	10.1	$(3.32 \pm 0.74 \pm 0.33) \times 10^{-5}$
$\mathcal{B}(\bar{B}^0 \rightarrow \bar{\Lambda}_c^- \Xi_c^+) \mathcal{B}(\Xi_c^+ \rightarrow pK^- \pi^+)$	7.32	9.53	5.3	...	1.82	13.3	$(5.27 \pm 1.51 \pm 0.69) \times 10^{-6}$
$\mathcal{B}(\Xi_c^+ \rightarrow \Xi^- \pi^+ \pi^+)$	4.23	11.7	...	4.5	...	13.2	$(2.86 \pm 1.21 \pm 0.38)\%$
$\mathcal{B}(\Xi_c^+ \rightarrow pK^- \pi^+)$	3.66	14.0	...	4.5	...	15.2	$(0.45 \pm 0.21 \pm 0.07)\%$
$\mathcal{B}(\Xi_c^+ \rightarrow pK^- \pi^+) / \mathcal{B}(\Xi_c^+ \rightarrow \Xi^- \pi^+ \pi^+)$	4.90	11.0	12.0	$0.16 \pm 0.06 \pm 0.02$

values obtained from the fits to the MC simulated signal distributions. The fit results are shown in Fig. 2.

The signal yields are $N_{\Xi^- \pi^+ \pi^+} = 24.2 \pm 5.4$ (6.9σ significance and 6.8σ with systematic uncertainties included) and $N_{pK^- \pi^+} = 24.0 \pm 6.9$ (4.5σ significance and 4.4σ with systematic uncertainties included). We use the efficiencies from MC simulations to measure $\mathcal{B}(\bar{B}^0 \rightarrow \bar{\Lambda}_c^- \Xi_c^+) \mathcal{B}(\Xi_c^+ \rightarrow \Xi^- \pi^+ \pi^+)$ and $\mathcal{B}(\bar{B}^0 \rightarrow \bar{\Lambda}_c^- \Xi_c^+) \mathcal{B}(\Xi_c^+ \rightarrow pK^- \pi^+)$ as $[3.32 \pm 0.74(\text{stat.})] \times 10^{-5}$ and $[5.27 \pm 1.51(\text{stat.})] \times 10^{-6}$, respectively.

We divide the above product branching fractions by the value of $\mathcal{B}(\bar{B}^0 \rightarrow \bar{\Lambda}_c^- \Xi_c^+)$ and for the first time measure $\mathcal{B}(\Xi_c^+ \rightarrow \Xi^- \pi^+ \pi^+)$, $\mathcal{B}(\Xi_c^+ \rightarrow pK^- \pi^+)$, and the ratio between them. These are listed in Table I.

There are several sources of systematic uncertainties in the branching fraction measurements. The uncertainties related to reconstruction efficiency include those for tracking efficiency (0.35% per track), particle identification efficiency (0.9% per kaon, 0.9% per pion, and 3.3% per proton), as well as Λ reconstruction efficiency (3.0% per Λ [41]). We assume these reconstruction-efficiency-related uncertainties are independent and sum them in quadrature. We estimate the systematic uncertainties associated with the fitting procedures by changing the order of the background polynomial, the range of the fit, and by enlarging the mass resolution by 10%. The observed deviations from the nominal fit results are taken as systematic uncertainties. The uncertainty on $\mathcal{B}(\bar{\Lambda}_c^- \rightarrow \bar{p}K^+\pi^-)$ is taken from Ref. [1]. The uncertainty due to the B^0 tagging efficiency is 4.5% [42]. A relative systematic uncertainty on $\mathcal{B}(\Upsilon(4S) \rightarrow B^0 \bar{B}^0)$ is 1.23% [1]. The systematic uncertainty on $N_{\Upsilon(4S)}$ is 1.37% [43]. For the Ξ_c^+ branching fractions and the corresponding ratio, some common systematic uncertainties, including tracking, particle identification, $\bar{\Lambda}_c^-$ decay branching fraction, Λ selection, and the total number of $B\bar{B}$ pairs, cancel. We summarize the sources of systematic uncertainties in Table I, assume them to be independent, and add them in quadrature to obtain the total systematic uncertainties.

We report the first measurements of the absolute branching fractions:

$$\mathcal{B}(\Xi_c^+ \rightarrow \Xi^- \pi^+ \pi^+) = (2.86 \pm 1.21 \pm 0.38)\%,$$

$$\mathcal{B}(\Xi_c^+ \rightarrow pK^- \pi^+) = (0.45 \pm 0.21 \pm 0.07)\%,$$

where the first uncertainties are statistical and the second systematic. The measured $\mathcal{B}(\Xi_c^+ \rightarrow \Xi^- \pi^+ \pi^+)$ value is consistent with the theoretical prediction within uncertainties [27]. The measured central value of $\mathcal{B}(\Xi_c^+ \rightarrow pK^- \pi^+)$ is smaller than that of the theoretical predictions [23,28], perhaps indicating a large U -spin symmetry breaking effect in the singly-Cabibbo-suppressed charmed-baryon decays. The branching fraction $\mathcal{B}(\bar{B}^0 \rightarrow \bar{\Lambda}_c^- \Xi_c^+)$ is measured for the first time to be $[1.16 \pm 0.42(\text{stat.}) \pm 0.15(\text{syst.})] \times 10^{-3}$ and agrees well with that of $B^- \rightarrow \bar{\Lambda}_c^- \Xi_c^0$ [16] which is consistent with the expectation from isospin symmetry. The product branching fractions are

$$\begin{aligned} \mathcal{B}(\bar{B}^0 \rightarrow \bar{\Lambda}_c^- \Xi_c^+) \mathcal{B}(\Xi_c^+ \rightarrow \Xi^- \pi^+ \pi^+) \\ = (3.32 \pm 0.74 \pm 0.33) \times 10^{-5}, \end{aligned}$$

$$\begin{aligned} \mathcal{B}(\bar{B}^0 \rightarrow \bar{\Lambda}_c^- \Xi_c^+) \mathcal{B}(\Xi_c^+ \rightarrow pK^- \pi^+) \\ = (5.27 \pm 1.51 \pm 0.69) \times 10^{-6}. \end{aligned}$$

The first of these branching fraction measurements is consistent with previous measurements, with improved precision, and supersedes the Belle measurement [30]. The ratio $\mathcal{B}(\Xi_c^+ \rightarrow pK^- \pi^+) / \mathcal{B}(\Xi_c^+ \rightarrow \Xi^- \pi^+ \pi^+)$ is measured to be $0.16 \pm 0.06(\text{stat.}) \pm 0.02(\text{syst.})$, which is consistent with world-average value of 0.21 ± 0.04 [1] within uncertainties. Our measured Ξ_c^+ branching fractions, e.g., for $\Xi_c^+ \rightarrow \Xi^- \pi^+ \pi^+$, can be combined with Ξ_c^+ branching fractions measured relative to $\Xi_c^+ \rightarrow \Xi^- \pi^+ \pi^+$ to yield other absolute Ξ_c^+ branching fractions.

In summary, based on $(772 \pm 11) \times 10^6$ $B\bar{B}$ pairs collected at the $\Upsilon(4S)$ resonance with the Belle detector, we perform an analysis of $\bar{B}^0 \rightarrow \bar{\Lambda}_c^- \Xi_c^+$ inclusively using a hadronic B -tagging method based on a full reconstruction algorithm [39], and exclusively with Ξ_c^+ decays into $\Xi^- \pi^+ \pi^+$ and $pK^- \pi^+$ final states. These are the first measurements of the absolute branching fractions $\mathcal{B}(\Xi_c^+ \rightarrow \Xi^- \pi^+ \pi^+)$ and $\mathcal{B}(\Xi_c^+ \rightarrow pK^- \pi^+)$.

ACKNOWLEDGMENTS

We thank Professor Fu-sheng Yu for useful discussions and comments. We thank the KEKB group for excellent operation of the accelerator; the KEK cryogenics group for efficient solenoid operations; and the KEK computer group, the NII, and PNNL/EMSL for valuable computing and SINET5 network support. We acknowledge support from MEXT, JSPS and Nagoya's the Tau-Lepton Physics Research Center (TLPRC) (Japan); ARC (Australia); FWF (Austria); National Natural Science Foundation of China (NSFC) under Contracts No. 11475187, No. 11521505, No. 11575017, No. 11761141009, and the Chinese Academy of Science Center for Excellence in Particle Physics (CCEPP) (China); MSMT (Czechia); the CarlZeiss

Foundation (CZF), DFG, the Excellence Cluster Universe (EXC153), and the VolkswagenStiftung (VS) (Germany); DST (India); INFN (Italy); MOE, MSIP, NRF, RSRI, Foreign Large-size Research Facility Application Supporting project (FLRFAS) project and GSDC of KISTI and Korea Research Environment Open Network (KREONET)/Global Ring Network for Advanced Application Development (GLORIAD)(Korea); MNiSW and NCN (Poland); Ministry of Science and Higher Education of the Russian Federation (MSHE), Grant No. 14.W03.31.0026 (Russia); ARRS (Slovenia); IKERBASQUE (Spain); SNSF (Switzerland); MOE and MOST (Taiwan); and DOE and NSF (USA).

-
- [1] M. Tanabashi *et al.* (Particle Data Group), *Phys. Rev. D* **98**, 030001 (2018).
- [2] B. Bhattacharya and J. L. Rosner, *Phys. Rev. D* **77**, 114020 (2008).
- [3] H. Y. Cheng and C. W. Chiang, *Phys. Rev. D* **81**, 074021 (2010).
- [4] H. N. Li, C. D. Lü, and F. S. Yu, *Phys. Rev. D* **86**, 036012 (2012).
- [5] S. Müller, U. Nierste, and S. Schacht, *Phys. Rev. D* **92**, 014004 (2015).
- [6] J. G. Körner, G. Krämer, and J. Wilrodt, *Z. Phys. C* **2**, 117 (1979).
- [7] T. Uppal, R. C. Verma, and M. P. Khanna, *Phys. Rev. D* **49**, 3417 (1994).
- [8] G. Kaur and M. P. Khanna, *Phys. Rev. D* **44**, 182 (1991).
- [9] Q. P. Xu and A. N. Kamal, *Phys. Rev. D* **46**, 270 (1992).
- [10] P. Zencykowski, *Phys. Rev. D* **50**, 402 (1994).
- [11] J. G. Körner and G. Krämer, *Z. Phys. C* **55**, 659 (1992).
- [12] H. Y. Cheng and B. Tseng, *Phys. Rev. D* **46**, 1042 (1992); Erratum **55**, 1697 (1997).
- [13] H. Y. Cheng and B. Tseng, *Phys. Rev. D* **48**, 4188 (1993).
- [14] A. Zupanc *et al.* (Belle Collaboration), *Phys. Rev. Lett.* **113**, 042002 (2014).
- [15] M. Ablikim *et al.* (BESIII Collaboration), *Phys. Rev. Lett.* **116**, 052001 (2016).
- [16] Y. B. Li *et al.* (Belle Collaboration), *Phys. Rev. Lett.* **122**, 082001 (2019).
- [17] M. J. Savage and R. P. Springer, *Phys. Rev. D* **42**, 1527 (1990).
- [18] R. Aaij *et al.* (LHCb Collaboration), *Phys. Rev. Lett.* **121**, 162002 (2018).
- [19] R. Aaij *et al.* (LHCb Collaboration), *Phys. Rev. Lett.* **121**, 072002 (2018).
- [20] R. Aaij *et al.* (LHCb Collaboration), *Phys. Rev. Lett.* **118**, 182001 (2017).
- [21] R. Aaij *et al.* (LHCb Collaboration), *Phys. Rev. Lett.* **121**, 162002 (2018).
- [22] R. Aaij *et al.* (LHCb Collaboration), *Phys. Rev. Lett.* **113**, 032001 (2014).
- [23] H. Y. Jiang and F. S. Yu, *Eur. Phys. J. C* **78**, 224 (2018).
- [24] S. Y. Jun *et al.* (SELEX Collaboration), *Phys. Rev. Lett.* **84**, 1857 (2000).
- [25] J. M. Link *et al.* (FOCUS Collaboration), *Phys. Lett. B* **512**, 277 (2001).
- [26] E. Vazquez-Jauregui *et al.* (SELEX Collaboration), *Phys. Lett. B* **666**, 299 (2008).
- [27] C. Q. Geng, Y. K. Hsiao, C. W. Liu, and T. H. Tsai, *Phys. Rev. D* **97**, 073006 (2018).
- [28] F. S. Yu, H.-Y. Jiang, R.-H. Li, C.-D. Lü, W. Wang, and Z.-X. Zhao, *Chin. Phys. C* **42**, 051001 (2018).
- [29] H. Y. Cheng, C. K. Chua, and S. Y. Tsai, *Phys. Rev. D* **73**, 074015 (2006).
- [30] R. Chistov *et al.* (Belle Collaboration), *Phys. Rev. D* **74**, 111105 (2006).
- [31] B. Aubert *et al.* (BABAR Collaboration), *Phys. Rev. D* **77**, 031101 (2008).
- [32] Inclusion of charge-conjugate states is implicit unless otherwise stated.
- [33] A. Abashian *et al.* (Belle Collaboration), *Nucl. Instrum. Methods Phys. Res., Sect. A* **479**, 117 (2002); also, see the detector section in J. Brodzicka *et al.*, *Prog. Theor. Exp. Phys.* (2012), 04D001 (2012).
- [34] S. Kurokawa and E. Kikutani, *Nucl. Instrum. Methods Phys. Res., Sect. A* **499**, 1 (2003), and other papers included in this volume; T. Abe *et al.*, *Prog. Theor. Exp. Phys.* **2013**, 03A001 (2013) and following articles up to 03A011.
- [35] D. J. Lange, *Nucl. Instrum. Methods Phys. Res., Sect. A* **462**, 152 (2001).
- [36] T. Sjöstrand, P. Edén, C. Friberg, L. Lönnblad, G. Miu, S. Mrenna, and E. Norrbin, *Comput. Phys. Commun.* **135**, 238 (2001).
- [37] R. Brun *et al.*, CERN Report No. DD/EE/84-1, 1984.
- [38] Y. B. Li *et al.* (Belle Collaboration), *Eur. Phys. J. C* **78**, 928 (2018).
- [39] M. Feindt, F. Keller, M. Kreps, T. Kuhr, S. Neubauer, D. Zander, and A. Zupanc, *Nucl. Instrum. Methods Phys. Res., Sect. A* **654**, 432 (2011).

- [40] H. Albrecht *et al.* (ARGUS Collaboration), *Phys. Lett. B* **229**, 304 (1989).
- [41] Y. Kato *et al.* (Belle Collaboration), *Phys. Rev. D* **94**, 032002 (2016).
- [42] A. Sibidanov *et al.* (Belle Collaboration), *Phys. Rev. D* **88**, 032005 (2013).
- [43] E. Guido *et al.* (Belle Collaboration), *Phys. Rev. D* **96**, 052005 (2017).